

Study of tunable band-gap properties in one-dimensional binary photonic crystals

FANG-CAO PENG^a, MING-YU JIANG^b, JIAN-WEI WU^{a*}

^aCollege of Physics and Electronic Engineering, Chongqing Normal University, Chongqing 401331, P.R. China

^bCollege of Computer and Information Science, Chongqing Normal University, Chongqing 401331, P.R. China

In this paper, the photonic band-gap of one-dimensional photonic crystals with $(AB)^N$ configuration is presented and thoroughly discussed based on transfer matrix method (TMM). Results show that band-gap properties including the width, central wavelength, and reflectance are directly related to refractive index, thickness, periodic number of dielectric materials, and incidence angle. By increasing the periodic number from 3 to 30, the reflectance is gradually enhanced till nearly stable. As both thickness ratio and refractive index ratio between two dielectric materials are increased, the band-gap width is remarkably extended. In addition, while the incidence angle is varied from 0° to 80° , the band-gap width is compressed (TM wave) and slightly broadened (TE wave), and the central wavelength of band-gap is shifted to shorter wavelength compared to the case of normal incidence.

(Received August 4, 2015; accepted February 10, 2017)

Keywords: Photonic crystals, Transfer matrix method, Photonic band-gap

1. Introduction

Based on the concept of a semiconductor crystals and electronic band-gap, S. John and E. Yablonovitch respectively put forward the concept of photonic crystals (PC) in 1987 [1, 2]. It is well-known that, in terms of the dimensionality of stacks, the photonic crystals can be classified into one-dimensional, two-dimensional, and three-dimensional structures. Because of these special arrangements, PC with periodic structure can easily control photons of electromagnetic wave, namely, the frequencies of photons within the band-gap can't exist through the photonic crystal, which is remarkably reflected [3-6]. As a consequence, photonic crystals will take on some significant properties resulting from band-gap compared to other devices so that the photonic crystals based waveguide have been attracted intensively attentions, and widely applied in various techniques such as slow light [7, 8], all-optical switch [9, 10], optical coupler [11, 12], laser [13-15], and sensor [16].

Based on previous reports, one can know that one-dimensional photonic crystal (1D PC) is often demonstrated in different applications due to its simple structure. Obviously, the photonic band-gap is an essential optical phenomenon in 1D PC, which has already been discussed in some literatures [17-19]. However, it is very significant to further research the band-gap of 1D PC for exploring its applications in various optical technologies. Therefore, in this study, the influence of physical parameters such as refractive index, dielectric thickness,

periodic number, and incidence angle on the band-gap of 1D PC will be presented and thoroughly investigated by means of transfer matrix method (TMM). Through this work, one can well-know the band-gap properties of 1D PC.

2. Theory model

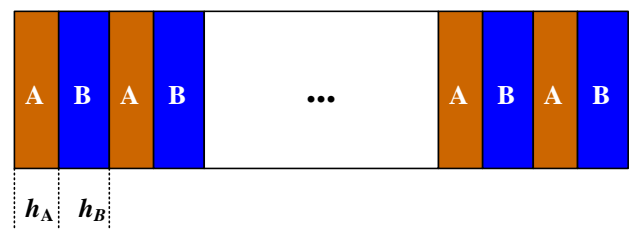


Fig. 1. The schematic diagram of one-dimensional binary photonic crystals with $(AB)^N$ configuration

One dimensional binary photonic crystal is made of two materials that are alternately arranged along one direction. The schematic diagram is shown in Fig. 1, where both A and B materials have different dielectric constants, ϵ_A and ϵ_B . The corresponding media thickness is, respectively, h_A and h_B shown in the schematic. Here, the refractive indexes of media A and B is, respectively, fixed at $n_A=2.35$, $n_B=1.38$ in this study. To simulate the electromagnetic wave propagation in photonic crystals, the

TMM technology that can connect the electric field and magnetic field component on both sides of the dielectric layer, that is presented as [20]

$$M_j = \begin{pmatrix} \cos \delta_j & -\frac{i}{\eta_j} \sin \delta_j \\ -i\eta_j \sin \delta_j & \cos \delta_j \end{pmatrix} \quad (1)$$

where the subscript j denotes the j th dielectric layer, the phase $\delta_j = (2\pi/\lambda)n_j h_j \cos \theta$, and $\eta_j = n_j \cos \theta$ (TE wave), or $\eta_j = n_j / \cos \theta$ (TM wave), θ is the incidence angle for each layer. If the total 1D PC is surrounded by air, θ_0 is the initial incidence angle for PC, $\cos \theta = \cos \theta_A = [1 - \sin^2 \theta_0 / (n_A)^2]^{1/2}$ for A media film, and $\cos \theta = \cos \theta_B = [1 - \sin^2 \theta_0 / (n_B)^2]^{1/2}$ for B media film.

Each the transfer matrix M_0 for AB unit can be written as

$$M_0 = M_A M_B \quad (2)$$

Full transfer matrix M of one-dimensional photonic crystals can be expressed by

$$M = (M_0)^N = \begin{pmatrix} M_{11} & M_{12} \\ M_{21} & M_{22} \end{pmatrix} \quad (3)$$

Using the matrix elements in Eq. (3), the reflectance coefficient of 1D PC is given by

$$r = \frac{(M_{11} + M_{12}\eta_{N+1})\eta_0 - (M_{21} + M_{22}\eta_{N+1})}{(M_{11} + M_{12}\eta_{N+1})\eta_0 + (M_{21} + M_{22}\eta_{N+1})} \quad (4)$$

where M_{mn} ($m, n=1, 2$) denotes the matrix elements, the coefficient $\eta_{N+1} = \eta_0 = \cos(\theta_0)$.

The corresponding power reflectivity is given by

$$R = |r|^2 \quad (5)$$

Based on above theoretical method, the photonic band-gap properties of 1D PC can be numerically researched by changing the parameters including repetition number, media thickness, refractive index, and incidence angle.

3. Results and discussion

Fig. 2 shows the photonic band-gap of 1D PC with changed repetition number, in which, under the condition of normal incidence, the TE wave is introduced into the photonic crystals, and the thickness of media A and B is, respectively, set to $h_A = 63.8$ nm, and $h_B = 108.7$ nm. As can be seen from the figure, in the case of $N=3$, the maximum

reflectivity is ~ 0.85 . It implies that energy of incident electromagnetic wave is spread through the photonic crystal. As a result, the band-gap of photonic crystals can not be observed in Fig. 2 (a). As the repetition number is increased to $N=5$, the maximum reflectivity is also enhanced to ~ 0.98 shown in Fig. 2 (b) with the result that the corresponding photonic band-gap is partly formed. While the repetition number is equal to 12, the full photonic band-gap illustrated in Fig. 2 (c) is achieved, which has steep band edges and flat top. The wavelength of referred bandwidth is from ~ 510 nm to ~ 740 nm, where the reflectivity is closed to $\sim 100\%$. It is obvious that the obtained photonic band-gap tends to stable state by further increasing the repetition number. The behaviors can be respectively observed for two cases of $N=20, 30$, in Fig. 2 (d) and (e). These phenomena can be explained by using the multi-beam optical coherence theory of multilayer stacks [20]. Based on the discussion, one can conclude that under a proper computation time condition, the repetition number should be judiciously selected to obtain an idea photonic band-gap.

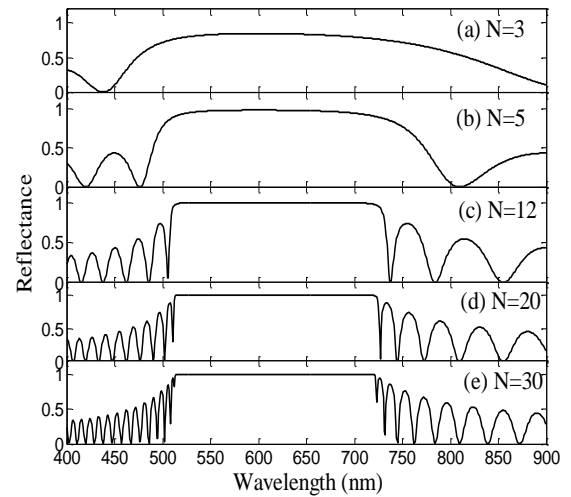


Fig. 2. Photonic band-gap for different repetition numbers

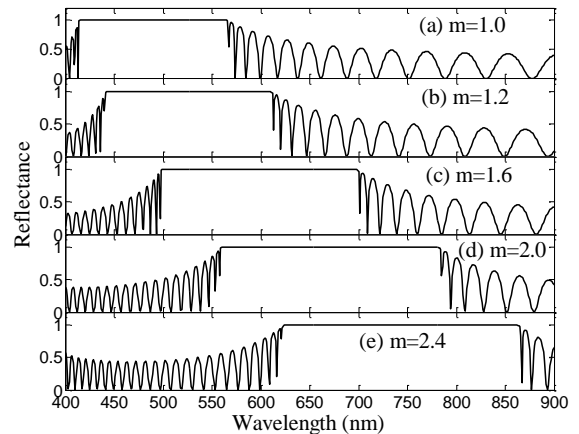


Fig. 3. Photonic band-gap with various thickness ratios

Fig. 3 plots the photonic band-gap with different thickness ratio for media A and B, in which the repetition number is $N=30$, and other parameters are identical to those of Fig. 2. The thickness ratio is defined by $m=h_B/h_A$, which is changed by increasing h_B , and fixing h_A in this plot. In Fig. 3 (a)~(e), one can see that, as the thickness ratio m is gradually increased from 1 to 2.4, the bandwidth is remarkably extended, and central wavelength of band-gap is shifted to longer wavelength. It is obvious that, because of the increase of the optical length for B layer as a result of the extended length of B layer, the resonance wavelengths supported by B layer are shifted to longer wavelengths so that the band-gap created by the combined effects of A and B layers is shifted to longer wavelength. As a consequence, the width of band-gap is also broadened. Therefore, while the thickness ratio m varies from 1 to 2.4, the corresponding bandwidth of photonic band-gap is significantly broadened from ~ 162 nm to ~ 229 nm, and the central wavelength is increased from ~ 525 nm to ~ 741 nm based on the combined actions of reflectivity wavelength of media A and B. Here, an interesting phenomenon is observed that the transmission on both sides of band-gap becomes asymmetrical with increase of thickness ratio. In addition, based on above discussion, another predictable behavior is that, if the referred thickness ratio m is increased by reducing the length of A layer, the width of band-gap will be compressed, and the central wavelength of the band-gap will also be shifted to shorter wavelength due to the reduced optical length. The corresponding results are not illustrated in this study.

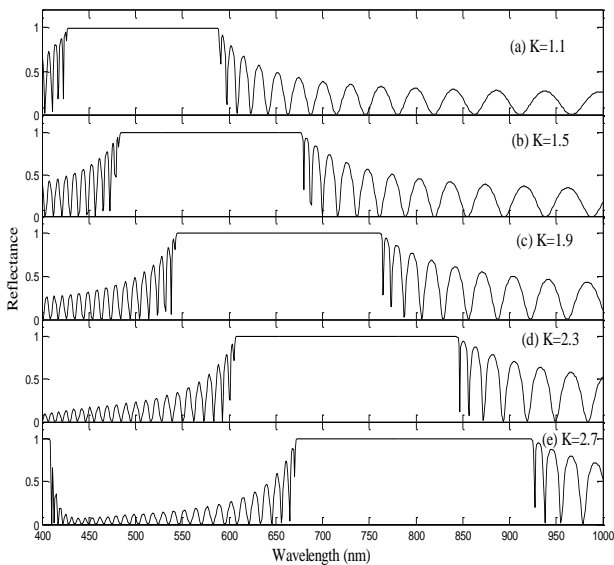


Fig. 4. Band-gap with different refractive index ratios

Fig. 4 shows the photonic band-gap with changed refractive index ratios that is defined by $K=n_A/n_B$, where other parameters are identical to those given in Fig. 3. In order to change K , the refractive index n_B is kept a constant, 1.38, and n_A is gradually increased. As the refractive index ratio is gradually increased from $K=1.1$ to 2.7, the bandwidth is also extended from ~ 150 nm to ~ 250 nm, and the band-gap center is shifted from ~ 500 nm to ~ 800 nm. In reality, the referred phenomena and the corresponding physical mechanisms are also similar to the case of Fig. 3. The resonance wavelengths of A layer is shifted to longer wavelength due to the enhanced optical length caused by the increased refractive index so that the band-gap is also red-shifted due to the enhanced effective refractive index in each AB unit that also extends the width of band-gap. In the investigation, one can find that, if the optical length produced by the product of refractive index and length is increased (decreased), the central wavelength of band-gap will be shifted to longer (shorter) wavelength. To clearly observe the variation of central wavelength and bandwidth of reflectivity band-gap against the n_A/n_B and h_B/h_A , the corresponding results are displayed in Fig. 5, in which both central wavelength and bandwidth are always linearly grown with the increase of ratios for n_A/n_B and h_B/h_A , i.e., the central wavelength is shifted to longer wavelength, and bandwidth is extended. However, it should be pointed out that, in Fig. 5 (b), the slope of red line with closed square marks is obviously large compared to the case of blue line with closed triangle marks. This implies that the bandwidth is easily broadened by increasing the refractive index ratio, and is not so sensitive to ratio of h_B/h_A .

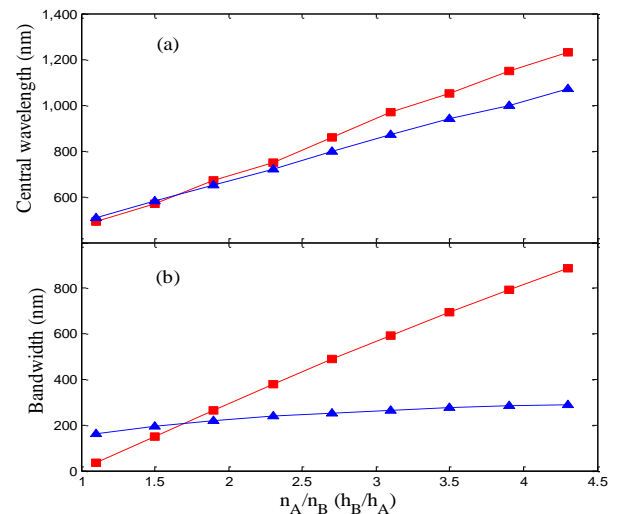


Fig. 5. (a) Central wavelength of band-gap, and (b) bandwidth as a function of n_A/n_B (red line with closed square marks) and h_B/h_A (blue line with closed triangle marks)

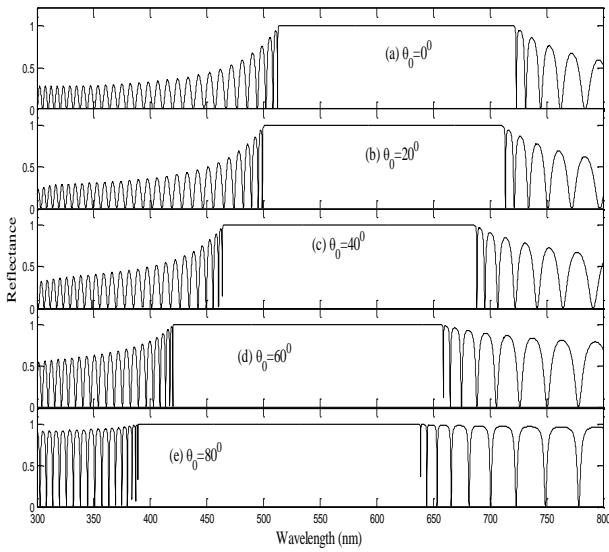


Fig. 6. Band-gap of TE wave with various incidence angles

In the case of oblique incidence, band-gap of TE and TM waves are, respectively, plotted with various incidence angles in Figs. 6 and 7, in which, $N=30$, and other parameters are same as those used in Fig. 2. From the figures, one can see that, as the incidence angle θ_0 is increased, their center wavelength is shifted to shorter wavelength because the effective optical length for reflected wavelengths is shortened resulting from the increased incidence angle. As a result, the corresponding resonance wavelengths are shifted to shorter wavelength for the larger incidence angle compared to the case of smaller incidence angle. Additionally, it is surprising that, the bandwidth of TE wave is slightly extended at larger incidence angle compared to the case of small incidence angle. Contrarily, while the incidence angle is increased to 80° , the corresponding bandwidth of TM wave is remarkably compressed to ~ 86 nm. However, as the incidence angle is reduced to the case of 0° , the bandwidth is quickly extended to ~ 209 nm. Based on the figures, one can conclude that the bandwidth of TM wave is very sensitive to the incidence angle. The more detailed variation is plotted in Fig. 8, where one can observe the normalized results of both central wavelength and bandwidth for TE and TM wave as the incidence angle is varied from 0° to 80° .

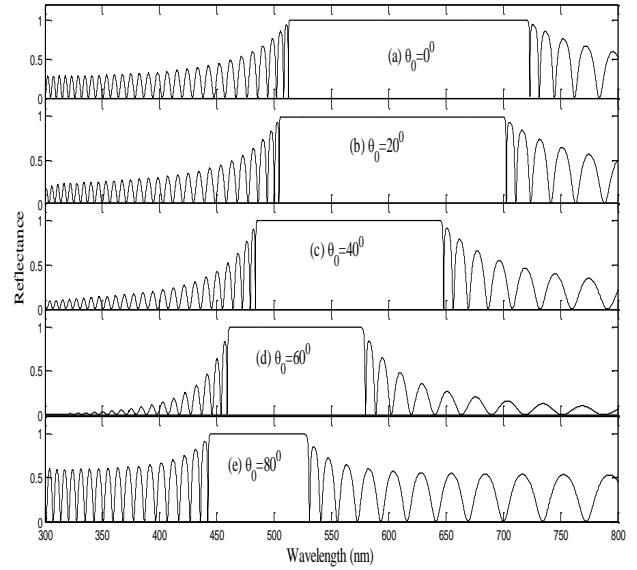


Fig. 7. Band-gap of TM wave with various incidence angles

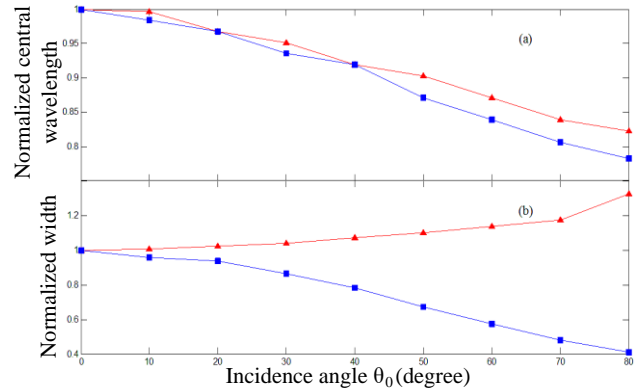


Fig. 8. (a) Normalized central wavelength and (b) normalized bandwidth of photonic band-gap for TE wave (red line with closed triangle marks) and TM wave (blue line with closed square marks) against initial incidence angle

4. Conclusions

By means of transfer matrix method, the band-gap properties of one-dimensional photonic crystals with $(AB)^N$ structure are presented and thoroughly discussed in this work. Enough repetition number for photonic crystals can lead to the full reflectivity band-gap. The refractive index ratio and thickness ratio of A and B layers strongly affect the bandwidth and central wavelength of achieved band-gap. In the case of oblique incidence, central position in band-gap is always shifted to shorter wavelength with increase of incidence angle. However, the width of band-gap is slightly extended (remarkably compressed) for TE wave (TM wave) for the larger incidence angle compared to the case of small incidence angle.

Acknowledgements

The authors acknowledge support from the National Natural Science Foundation of China (Grant no. 61205111), Scientific and Technological Research Program of Chongqing Municipal Education Commission (Grant no. KJ130633), and Postdoctoral Science Foundation of China (Grant no. 2014M562293).

References

- [1] S. John, *Phys. Rev. Lett.* **58**, 2486 (1987).
- [2] E. Yablonovitch, *Phys. Rev. Lett.* **58**, 2059 (1987).
- [3] J. X. Liu, Z. K. Yang, H. W. Yang, Q. K. Xi, A. P. Li, X. You, *J. Russ. Laser Res.* **34**, 262 (2013).
- [4] H. F. Zhang, S. B. Liu, Y. C. Jiang, *J. Plasma Phys.* **81**(2): 905810201, (2015).
- [5] L. Wang, L. G. Wang, *Phys. Lett. A* **379**, 1847 (2015).
- [6] E. H. Khoo, T. H. Chen, A. Q. Liu, J. Li, D. Pinjala, *Appl. Phys. Lett.* **91**, 171109 (2007).
- [7] X. Zhang, H. P. Tian, Y. F. Ji, *Opt. Commun.* **283**, 1768 (2010).
- [8] D. L. Su, S. L. Pu, W. Z. Lei, *J. Optoelectron. Adv. M.* **18**, 453 (2016).
- [9] T. Tanabe, M. Notomi, S. Mitsugi, A. Shinya, E. Kuramochi, *Opt. Lett.* **30**, 2575 (2005).
- [10] Y. H. Lu, M. D. Huang, S. Y. Park, P. J. Kim, Y. P. Lee, J. Y. Rhee, *J. Korean Phys. Soc.* **51**, 1550 (2007).
- [11] K. Hennessy, C. Reese, A. Badolato, C. F. Wang, A. Imamoglu, P. M. Petroff, E. Hu, G. Jin, S. Shi, D. W. Prather, *Appl. Phys. Lett.* **83**, 3650 (2003).
- [12] A. Faraon, E. Waks, D. Englund, J. Vuckovic, *Appl. Phys. Lett.* **90**, 073102 (2007).
- [13] H. Altug, J. Vuckovic, *Opt. Express* **13**, 8819 (2005).
- [14] J. C. Knight, *J. Opt. Soc. Am. B* **24**, 1661 (2007).
- [15] B. Liu, Y. F. Liu, S. J. Li, X. D. He, *Opt. Commun.* **368**, 7 (2016).
- [16] S. Jindal, S. Sobti, M. Kumar, S. Sharma, M. K. Pal, *IEEE Sens. J.* **16**, 3705 (2016).
- [17] C. Isaac Angert, S. K. Remillard, *Micro. Opt. Technol. Lett.* **51**, 1010 (2009).
- [18] R. L. Wang, J. Zhang, Q. F. Hu, *J. Korean Phys. Soc.* **52**, S71 (2008).
- [19] S. Makino, T. Fujisawa, K. Saitoh, *IEEE Photon. J.* **7**, 4501608 (2015).
- [20] M. Born, E. Wolf, *Principle of Optics, Seventh Edition*, United Kingdom: Cambridge University Press (2013).

*Corresponding author: jwwu@uestc.edu.cn